Effects of the vibrational and rotational excitation of reagent on the stereodynamics of the reaction S (^{3}P) + H_2 → SH + H*

Shan Guang-Ling(单广玲), Wang Mei-Shan(王美山)†, Yang Chuan-Lu(杨传路), and Li Yan-Qing(李艳青)

School of Physics and Optoelectronic Engineering, Ludong University, Yantai 264025, *China*

(Received 7 September 2013; revised manuscript received 29 November 2013; published online 10 April 2014)

Quasiclassical trajectory (QCT) calculations are first carried out to study the stereodynamics of the S (^{3}P) + H_2 → SH + H reaction based on the *ab initio* $1^3A''$ potential energy surface (PES) (Lü *et al.* 2012 *J. Chem. Phys.* **136** 094308). The QCT-calculated reaction probabilities and cross sections for the S + H_2 ($v = 0$, $j = 0$) reaction are in good agreement with the previous quantum mechanics (QM) results. The vector properties including the alignment, orientation, and polarization-dependent differential cross sections (PDDCSs) of the product SH are presented at a collision energy of 1.8 eV. The effects of the vibrational and rotational excitations of reagent on the stereodynamics are also investigated and discussed in the present work. The calculated QCT results indicate that the vibrational and rotational excitations of reagent play an important role in determining the stereodynamic properties of the title reaction.

Keywords: stereodynamics, QCT method, vector correlation, vibrational and rotational excitation

PACS: 82.30.Cf, 82.20.Fd, 82.20.Hf, 82.20.Kh **DOI:** 10.1088/1674-1056/23/6/068201

1. Introduction

As is well known, sulfur and sulfur-containing species play an important role in atmospheric and combustion chemistry, specifically, the reaction S (^{3}P) + H_2 → SH + H is the simplest reaction involving sulfur atoms and can provide the prototype for one to study the hydrogen-atom abstraction reaction, which features an activation barrier on the reaction path. The reaction S (^{3}P) + H_2 is less extensively investigated in contrast to the analogous reaction O (^{3}P) + H_2 which has been well studied both experimentally and theoretically.[1–4] Therefore, the extensive theoretical studies of the title reaction are significant and necessary.

In previous studies, three triplet electronic states ($1^3A''$, $2^3A''$, $1^3A'$) for the title reaction were reported[5–7] and more attention was focused on the singlet-triplet crossing effect[6,8–10] which usually occurred in the entrance channel. In 1983, Martin[5] reported on the first potential energy surface (PES) for the reaction H + HS. The determined transition state was found to be linear with $R_{HS} = 2.6a_0$ and $R_{HH} = 2.6a_0$. In 2004, Maiti *et al.*[6] constructed the PESs of the two lowest triplet states of SH_2 ($^3A''$ and $^3A'$) to study the intersystem crossing effects on the S (^{1}D,^{3}P) + H_2 → HS + H reaction and performed the trajectory surface-hopping calculation. The three-dimensional (3D) spline interpolation method was employed to construct the PES in the interaction areas and a London–Eyring–Polanyi–Sato (LEPS) function was used to construct the PES in the asymptotic areas. They found that the intersystem crossing effect on the thermal rate constant at low temperature was very important. Then, Klos *et al.*[7] constructed an analytical PES of H_2S ($^3A''$) based on the internally contracted multi-reference configuration interaction (MRCI) with single and double excitation level including the Davidson's correction with the aug-cc-pVQZ (AVQZ) basis set. Recently, Lü *et al.*[11] obtained a new high-quality Lü–Zhang–Han–He (LZHH) PES for the lowest triplet state of H_2S ($^3A''$) at the MRCI/aug-cc-pV5Z level. Furthermore, they presented an exact quantum dynamical study and QCT calculations for the reaction probability and cross section of the H + HS reaction. Besides, Lü *et al.*[12] carried out the quantum scattering dynamic calculation of the title reaction using the time-dependent wave-packet method. They found that both vibrational and rotational excitation enhance the reactivity of the title reaction. However, what is the influence of the vibration and rotational excitation on the stereodynamics of the title reaction? No group has answered this question so far. In the present work we employ the QCT method to investigate the influence of vibration and rotational excitation on the stereodynamics of the title reaction based on the new LZHH $^3A''$ PES.[11]

The rest of this paper is organized as follows. In Section 2, we briefly describe the main features of the H_2S ($^3A''$) potential as well as the QCT calculation. The detailed results and discussion are presented in Section 3. Finally, the main conclusions are drawn from the present study in Section 4.

*Project supported by the National Natural Science Foundation of China (Grant Nos. 11074103, 10974078, and 11174117) and the Discipline Construction Fund of Ludong University, China.

†Corresponding author. E-mail: mswang1971@163.com

© 2014 Chinese Physical Society and IOP Publishing Ltd

2. PES and QCT calculation

2.1. Potential energy surface

The QCT[13,14] calculations have been performed on the $^3A''$ SH_2 *ab initio* PES constructed by Lü *et al.*[11] The *ab initio* single-point energies are calculated using the complete active space self-consistent field (CASSCF)[15,16] method and the multi-reference configuration interaction (MRCI)[17–19] method by the MOLPRO package[20] with the aug-cc-pV5Z (AV5Z) basis set.[21] The main topographical features relevant to the title reaction are given in Fig. 1.[12] From Fig. 1, one can clearly see the energy profile along the minimum energy reaction pathway of the title reaction. There exists a barrier of 1.043 eV on the reaction path, and the endoergicity, considering the zero point energy, is 0.854 eV. For more details of the PES, readers can refer to Ref. [11].

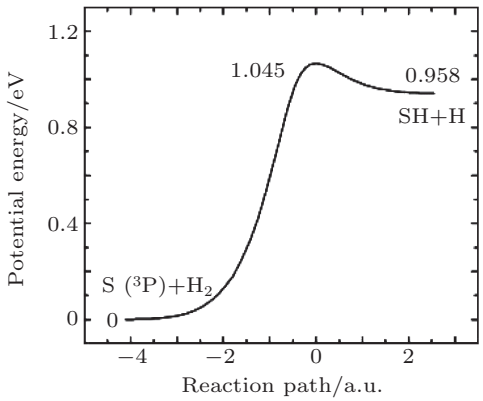


Fig. 1. Energy profile along the minimum energy reaction pathway for the title reaction (cited from Ref. [11]).

2.2. Quasi-classical trajectory calculations

A benchmark QCT procedure provided by Han's group is used in the present work. The QCT procedure has been successfully carried out in many reaction systems.[22–27] In our calculation, the integration step is chosen to be 0.1 fs, which can ensure the good convergence of the results. In order to ensure no interaction between attacking atom H and the center-of-mass (CM) of the molecule H_2, the distance between them is set to be 20 Å. A branch of 10^5 trajectories is run for each rovibrational state of the title reaction. The collision energy is set to be 1.8 eV for the present calculations and the rovibrational state of the reagent H_2 molecule has $v = 0$–3 and $j = 0$–3. The orientation of the diatomic molecule and the phase of the diatomic vibrational motion are randomly sampled by a Monte Carlo method. The impact parameters are optimized before running the trajectories. In the QCT framework, the total reactive probability, N_r/N_T, is the ratio of the number of reactive trajectories to the total number of trajectories. The reactive cross section is given by

$$\sigma_r = \pi b_{max}^2 \frac{N_r}{N_T}, \tag{1}$$

where b_{max} is the maximum value of the impact parameter b. That is to say, if b is larger than b_{max}, then there are no reaction trajectories in the region of $b_{max} - b$.

2.3. Vector correlation

Figure 2 illustrates the CM reference frame used in the present investigation. The reagent initial relative velocity vector $\boldsymbol{k}$ is parallel to the z axis of the CM frame. The scattering plane (x–z plane) contains $\boldsymbol{k}$ and relative velocity vector $\boldsymbol{k}'$ of final product. The scattering angle θ_t is the angle included between $\boldsymbol{k}$ and $\boldsymbol{k}'$. θ_r and ϕ_r are the polar and azimuthal angles of the final rotational angular momentum $\boldsymbol{j}'$, respectively.

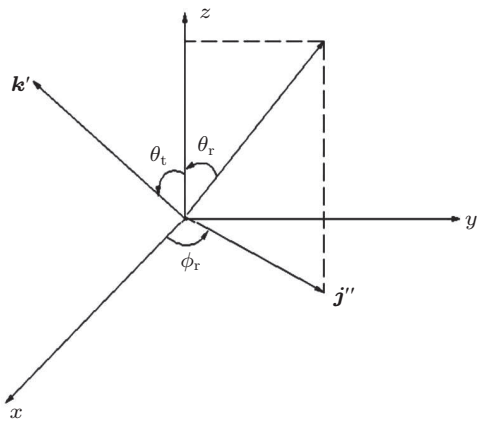


Fig. 2. CM coordinate system used to describe the $\boldsymbol{k}$–$\boldsymbol{k}'$–$\boldsymbol{j}'$ correlations.

The distribution function $P(\theta_r)$ describing the $\boldsymbol{k}$–$\boldsymbol{j}'$ correlation can be expanded in a series of Legendre polynomials[28]

$$P(\theta_r) = \frac{1}{2}\sum_k (2k+1) a_0^{(k)} P_k(\cos\theta_r). \tag{2}$$

The expansion coefficient

$$a_0^{(k)} = \int_0^{\pi} P(\theta_r) P_k(\cos\theta_r) \sin\theta_r \, d\theta_r = \langle P_k(\cos\theta_r)\rangle \tag{3}$$

is the polarization parameter. When k is odd, $a_0^{(k)}$ is called the orientation parameter, and when k is even it is called the alignment parameter. As $k = 2$, the expansion coefficient,

$$a_0^{(2)} = \langle P_2(\cos\theta_r)\rangle = \langle P_2(j\cdot k)\rangle = \frac{1}{2}\left\langle 3\cos^2\theta_r - 1\right\rangle \tag{4}$$

which gives a simple way to express the degree of the product rotational alignment, is called the rotational alignment parameter of the product.

The dihedral angle distribution function $P(\phi_r)$ describing the $\boldsymbol{k}$–$\boldsymbol{k}'$–$\boldsymbol{j}'$ correlation can be expanded in a Fourier series[28]

$$P(\phi_r) = \frac{1}{2\pi}\left(1 + \sum_{\text{even},n\geq 2} a_n \cos n\phi_r + \sum_{\text{even},n\geq 1} b_n \sin n\phi_r\right), \tag{5}$$

where

$$a_n = 2\langle \cos n\phi_r\rangle \quad \text{and} \quad b_n = 2\langle \sin n\phi_r\rangle. \tag{6}$$

In the present work, in order to show a good convergence the $P(\phi_r)$ distribution is expanded up to $n = 24$.

The resulting probability density function of angles θ_r and ϕ_r can be expressed by

$$\begin{aligned} & P(\theta_r, \phi_r) \\ = & \frac{1}{4\pi} \sum_{kq} [k] a_q^k C_{kq}(\theta_r, \phi_r)^* \\ = & \frac{1}{4\pi} \sum_{k} \sum_{q \geq 0} \left[a_{q\pm}^k \cos q\phi_r - a_{q\mp}^k \sin q\phi_r \right] C_{kq}(\theta_r, 0). \end{aligned} \quad (7)$$

The polarization parameter is expressed as

$$a_{q\pm}^k = 2 \left\langle C_{k|q|}(\theta_r, 0) \cos q\phi_r \right\rangle, \quad k \text{ is even}, \quad (7a)$$

$$a_{q\mp}^k = 2i \left\langle C_{k|q|}(\theta_r, 0) \sin q\phi_r \right\rangle, \quad k \text{ is odd}. \quad (7b)$$

In this work, in order to show a good convergence, the $P(\theta_r, \phi_r)$ distribution is expanded up to $k = 7$.

The fully correlated angular distribution can be written as[24,29]

$$P(\omega_t, \omega_r) = \sum_{kq} \frac{[k]}{4\pi} \frac{1}{\sigma} \frac{d\sigma_{kq}}{d\omega_t} C_{kq}(\theta_r, \phi_r)^*. \quad (8)$$

Here, $[k] = 2k + 1$, $(1/\sigma)(d\sigma_{kq}/d\omega_t)$ is the generalized polarization-dependent differential cross section (PDDCS), and $C_{kq}(\theta_r, \phi_r)$ refers to the modified spherical harmonics. In the present work, four PDDCSs are taken into account, i.e., $(2\pi/\sigma)(d\sigma_{00}/d\omega_t)$, $(2\pi/\sigma)(d\sigma_{20}/d\omega_t)$, $(2\pi/\sigma)(d\sigma_{22+}/d\omega_t)$, and $(2\pi/\sigma)(d\sigma_{21-}/d\omega_t)$, which will be denoted as PDDCSs$_{00}$, PDDCSs$_{20}$, PDDCSs$_{22+}$, and PDDCSs$_{21-}$ respectively.

3. Results and discussion

In order to test the validity of the QCT method in the title reaction, we compare our QCT results of the reaction probability and the reaction cross section with the corresponding TDWP results[12] given by Lü *et al.*

Figure 3 presents the reaction probability of the reaction S (^{3}P) + H_2 ($v = 0$, $j = 0$) as a function of collision energy. One can see the threshold energy of the title reaction is about 0.9 eV, and the reaction probabilities tend to increase monotonically with the increasing of collision energy. The QCT results are slightly bigger than the quantum results at some collision energies, however, the QCT values are in good agreement with the quantum results on the whole. The calculated reaction cross section for $v = 0$, $j = 0$ as a function of collision energy, which is shown in Fig. 4. Both the centrifugal-sudden (CS) approximation and coupled-channel (CC) results[12] are also shown in Fig. 4. One can clearly see that the reaction cross section increases with the increase of collision energy. In addition, the CS results are smaller than the CC results in the high-energy region and the QCT results of this work are more consistent with the CC values. The above phenomenon can be explained by the simple feature of the PES: there are a straight uphill route and downhill route in S (^{3}P) + H_2 → HS + H reaction which can be seen in Fig. 1 and a direct reaction should take place. As is well known, the QCT method has a shortage of its inability to properly treat the quantum-mechanical effects, such as quantum resonance, quantum interference, tunneling, etc. Remarkable consistency between the QCT and quantum results here indicates that the quantum effect in the title reaction can be negligible. Therefore, one can conclude that the QCT calculations for the title reaction are reliable. It is easy to find that there is a straight uphill route and downhill route in the PES of S (^{3}P) + H_2 → HS + H reaction, and the reaction probability increases monotonically with the increasing of collision energy. Moreover, the values of probability and reaction cross section are quite small when the collision energy is below 1.0 eV. Therefore, we only focus our attention on the stereo-dynamics of the title reaction at the middle energy $E_{col} = 1.8$ eV in the present study. The effects of other collision energies on the stereo-dynamics of the title reaction can be found in our future work.

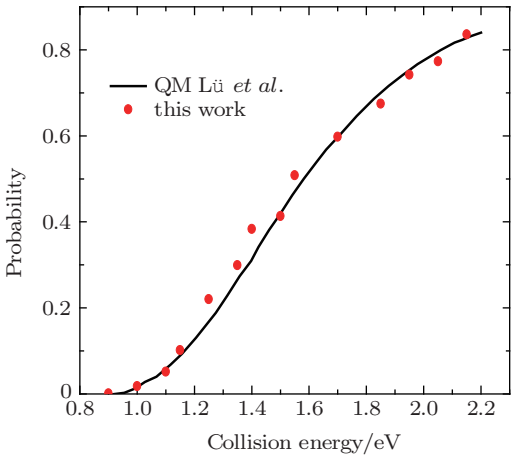


Fig. 3. (color online) Comparison of the reaction probability between our QCT result and TDWP calculations[12] for the S (^{3}P) + H_2($v = 0$, $j = 0$) reaction in a collision energy range of 0.9 eV–2.2 eV.

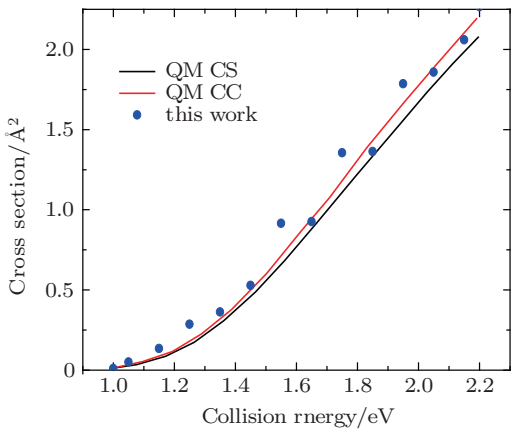


Fig. 4. (color online) Comparison of reaction cross section between our QCT result and TDWP calculations[12] for the S (^{3}P) + H_2 ($v = 0$, $j = 0$) reaction in a collision energy range of 0.9 eV–2.2 eV.

The $P(\theta_r)$ distributions can describe the $\boldsymbol{k}$–$\boldsymbol{j}'$ correlation and reflect the rotational polarization of the product. The $P(\theta_r)$ distributions for the S + H_2 ($v = 0$, $j = 0$–3) → HS + H reaction at $E_{col} = 1.8$ eV are shown in Fig. 5(a). Clearly, the $P(\theta_r)$ peaks are close to 90° and symmetric with respect to 90° for $j = 0$, 1 , 2 or 3, which means that the product rotational angular momentum vector $\boldsymbol{j}'$ is strongly aligned along the direction perpendicular to the $\boldsymbol{k}$ vector. It is obviously seen that the peaks of $P(\theta_r)$ distribution decrease as rotational angular momentum increases from 0 to 3, which shows that the alignment degree of the product decreases at the higher rotational excitation. The $P(\theta_r)$ distributions at different vibrational states ($j = 0$, $v = 0$, 1, 2, and 3) are depicted in Fig. 5(b). As shown in Fig. 5(b), the $P(\theta_r)$ distributions become lower and broader as the vibrational excitation increases, which means that the alignment degree of the product becomes weaker when the reagent is in the higher excited vibrational state. The alignment parameter $\langle P_2(\boldsymbol{j}' \cdot \boldsymbol{k})\rangle$ is another way to express the degree of product rotational polarization. As is well known, when the value of $\langle P_2(\boldsymbol{j}' \cdot \boldsymbol{k})\rangle$ is close to −0.5, $\boldsymbol{j}'$ is preferentially polarized and perpendicular to the reagent relative velocity. One can clearly see that the calculated values of $\langle P_2(\boldsymbol{j}' \cdot \boldsymbol{k})\rangle$, shown in Table 1, are consistent with the $P(\theta_r)$ distributions.

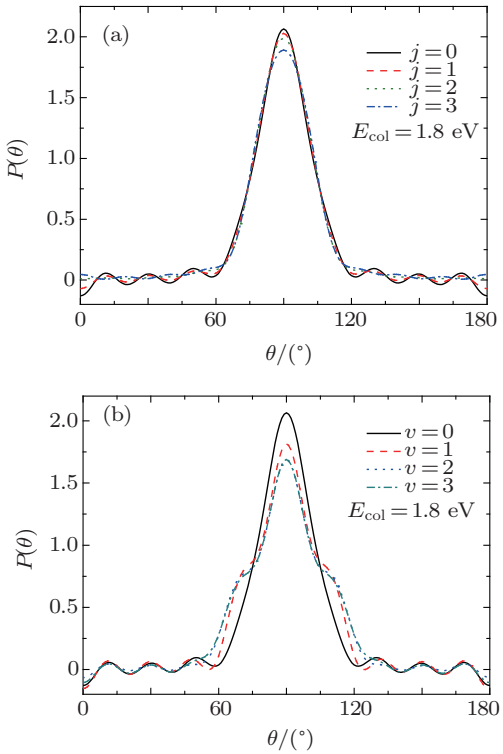


Fig. 5. (color online) Distributions of $P(\theta_r)$ for the reactions S (^{3}P) + H_2 (v, j) → HS + H at $E_{col} = 1.8$ eV. (a) $v = 0$, $j = 0$–3; (b) $v = 0$–3, $j = 0$.

Table 1. Calculated values of rotational alignment parameter of product for initial rotation and vibration states $v = 0$, $j = 0$–3 and $v = 0$–3, $j = 0$.

State (v, j)	(0, 0)	(0, 1)	(0, 2)	(0, 3)	(1, 0)	(2, 0)	(3, 0)
$\langle P_2(\boldsymbol{j}' \cdot \boldsymbol{k})\rangle$	–0.427	–0.426	–0.424	–0.418	–0.409	–0.392	–0.391

The $P(\phi_r)$ distributions describing the $\boldsymbol{k}$–$\boldsymbol{k}'$–$\boldsymbol{j}'$ correlations for the title reaction at E_{col} =1.8 eV are depicted in Fig. 6. Figure 6(a) corresponds to the $P(\phi_r)$ distributions for $v = 0$, $j = 0$–3, and Fig. 6(b) for $v = 0$–3, $j = 0$. The $P(\phi_r)$ distributions are asymmetric with respect to the $\boldsymbol{k}$–$\boldsymbol{k}'$ scattering plane (or about $\phi_r = 180°$). A conspicuous peak appears at $\phi_r = 270°$ for all the rotational and vibration states, which indicates a marked product alignment along the y axis and a marked product orientation pointing to the negative direction of the y axis, which implies that there exists a preference for the right-hand rotation of the product in the plane, which is parallel to the scattering plane. We use the term "out-of-planes" to refer to the preference of the product molecule to rotate in the plane which is perpendicular to the scattering plane, and the term "in-plane" to refer to the preference of the product molecule to rotate in the plane which is parallel to the scattering plane. The comparisons of $P(\phi_r)$ distributions between the different rotational and vibrational states reveal that the peaks of the $P(\phi_r)$ distribution at $\phi_r = 270°$ become broader, which indicates that the rotation of the product HS has a preference of changing from the in-plane reaction mechanism to the out-of-plane's mechanism with the increasing of the rovibrational excitation. The same phenomena can be found in the O (^{3}P) + H_2 reaction.[30]

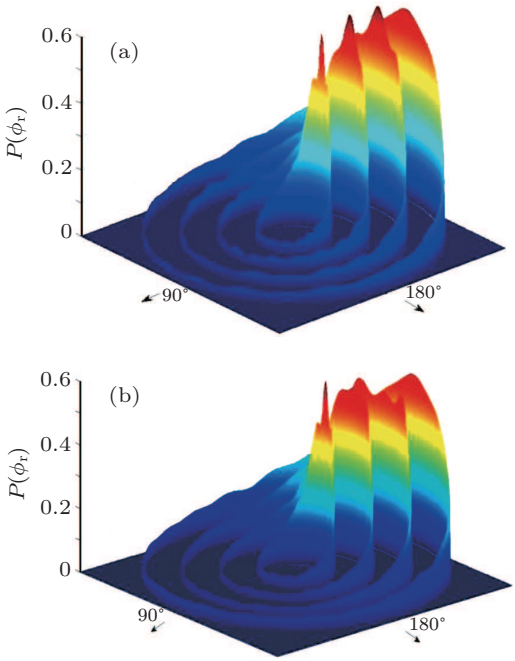


Fig. 6. (color online) Distributions of $P(\phi_r)$ for the reactions S (^{3}P) + H_2 (v, j) → HS + H at $E_{col} = 1.8$ eV. (a) $v = 0$, $j = 0$–3 (from inner to outer); (b) $v = 0$–3 (from inner to outer), $j = 0$.

In the above discussion, the $P(\theta_r)$ distribution is symmetric with respect to $\theta_r = 90°$ while the $P(\phi_r)$ distribution is asymmetric with respect to the $\boldsymbol{k}$–$\boldsymbol{k}'$ scattering plane. The

same phenomena can be found in the O (^{3}P) + H_2 reaction,[31] which can be explained by the proposed impulse model for a triatomic system.[14] In this model, the relationship between the product angular momentum $\boldsymbol{j}'$ with the orbital angular momentum $\boldsymbol{L}$ of reagent and the angular momentum $\boldsymbol{j}$ of reagent is described by a formula

$$\boldsymbol{j}' = \boldsymbol{L}\sin^2\beta + \boldsymbol{j}\cos^2\beta + \boldsymbol{J}_1 m_B/m_{AB},$$

where $\boldsymbol{J}_1 = \sqrt{\mu_{BC}E_r}(\boldsymbol{r}_{AB} \times \boldsymbol{r}_{BC})$, E_r is the repulsive energy, $\boldsymbol{r}_{AB}$, and $\boldsymbol{r}_{BC}$ are the unit vectors with B pointing to A and C, and μ_{BC} is the reduced mass of BC molecule. The first two terms $\boldsymbol{L}\sin^2\beta + \boldsymbol{j}\cos^2\beta$ on the right–hand side in the formula are symmetric, while the third term $\boldsymbol{J}_1 m_B/m_{AB}$ is asymmetric due to the effect of the repulsive energy. Therefore, the third term forms the asymmetric feature and leads to the preferred orientation of the angular momentum of product in the title reaction.

The PDDCSs for the reaction S (^{3}P) + H_2 → HS + H are present in Figs. 7 and 8. The $PDDCS_{00}$ is also called the differential cross section (DCS), and the $PDDCS_{20}$ correlates with the expectation value of the second Legendre moment $\langle P_2(\cos\theta_r)\rangle$. It is observed that $PDDCS_{20}$ displays an opposite trend to that of $PDDCS_{00}$ within the whole range of the scattering angles. The $PDDCSs_{00}$ (in Fig. 7(a)) indicates that the title reaction prefers both sideways scattering and backward scattering for the rotational excitation from $j = 0$ to 3. In other words, the degree of the backward scattering increases and the degree of the sideways scattering decreases as the value of j increases. From the opposite trends shown by $PDDCS_{20}$ (in Fig. 7(b)) and $PDDCS_{00}$, it can be inferred that the product angular momentum $\boldsymbol{j}'$ is strongly aligned along the direction perpendicular to k. In Fig. 7(c), it is obvious that the values of $PDDCSs_{22+}$ are all negative for almost all scattering angles, which indicates the remarkable preference for the product alignment along the y axis. Moreover, the polarization trends of the title reaction with the different rotational quantum numbers are similar, and all the strong polarizations of the products appear at about $\theta_t = 80°$ and $\theta_t = 150°$. The degree of polarization for the reaction becomes weaker with the increase of rotational quantum number. The $PDDCSs_{21-}$ is related to the average value $\langle \sin 2\theta_r \cos\phi_r\rangle$. From Fig. 7(d), one can see that the values of $PDDCSs_{21-}$ for the title reaction are negative in an angle range of 60°–180°, showing that the product rotational angular momentum $\boldsymbol{j}'$ is aligned along the direction of vector x–z in the sideways and backward hemisphere. Moreover, as the rotational quantum number increases, the degree of this alignment becomes weaker. We also find that the values of $PDDCSs_{21-}$ are close to zero in an angle range of 0°–60°, indicating no obvious effect of the reagent rotational excitation on $PDDCSs_{21-}$ in the forward hemisphere.

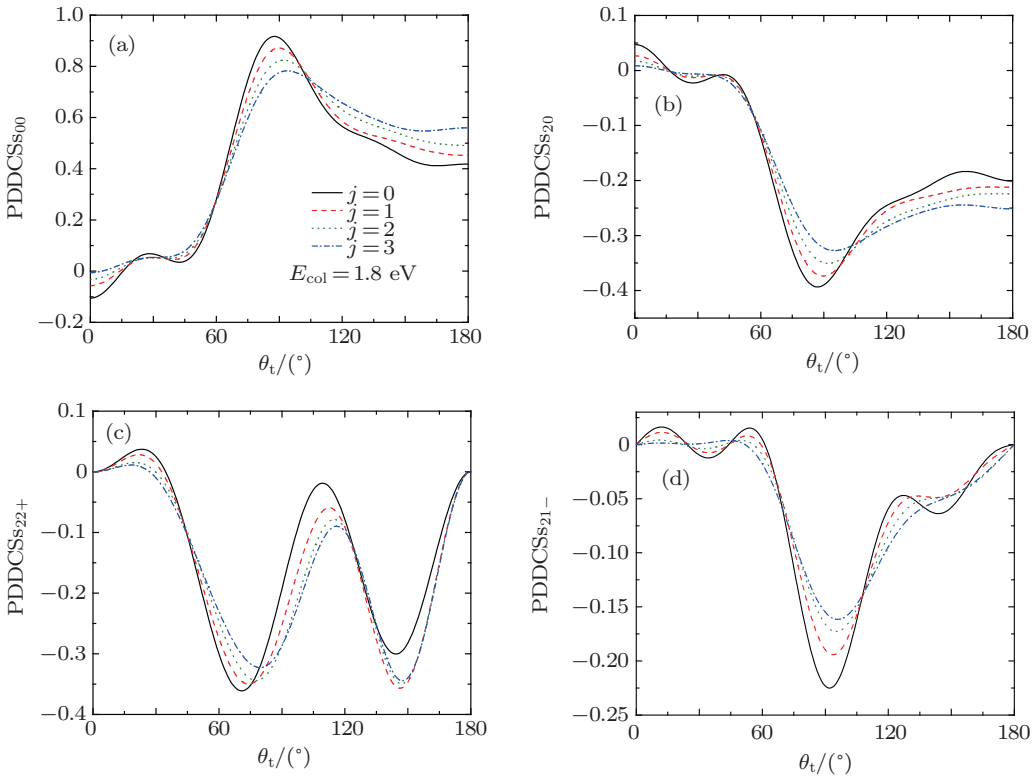


Fig. 7. (color online) Polarization-dependent differential cross sections for the reactions S (^{3}P) + H_2 ($v = 0$, $j = 0$–3) → HS + H at $E_{col} = 1.8$ eV. (a) $PDDCSs_{00}$, (b) $PDDCSs_{20}$, (c) $PDDCSs_{22+}$, (d) $PDDCSs_{21-}$.

As depicted in Figs. 8(a) and 8(b), one can conclude that the product vibration excitation has a positive effect on the $PDDCS_{20}$ and $PDDCS_{00}$. That is to say, the title reaction prefers the forward scattering for the vibrational excitation from $v = 0$ to 3, thereby affirming that the scattering direction is highly sensitive to the vibration excitation of reagent. In addition, the vibration quantum number has a strong influence on the angular distribution of PDDCSs with $q \neq 0$. In Fig. 8(c) the value of $PDDCSs_{22+}$ indicates that the degree of polarization for the reaction becomes stronger with the increase of the vibration quantum number. The distribution of $PDDCSs_{21-}$ is shown in Fig. 8(d). the strongest polarization degrees of the products of $v = 0$, 1, 2, and 3 are about 90°, 75°, 70°, and 50°, respectively.

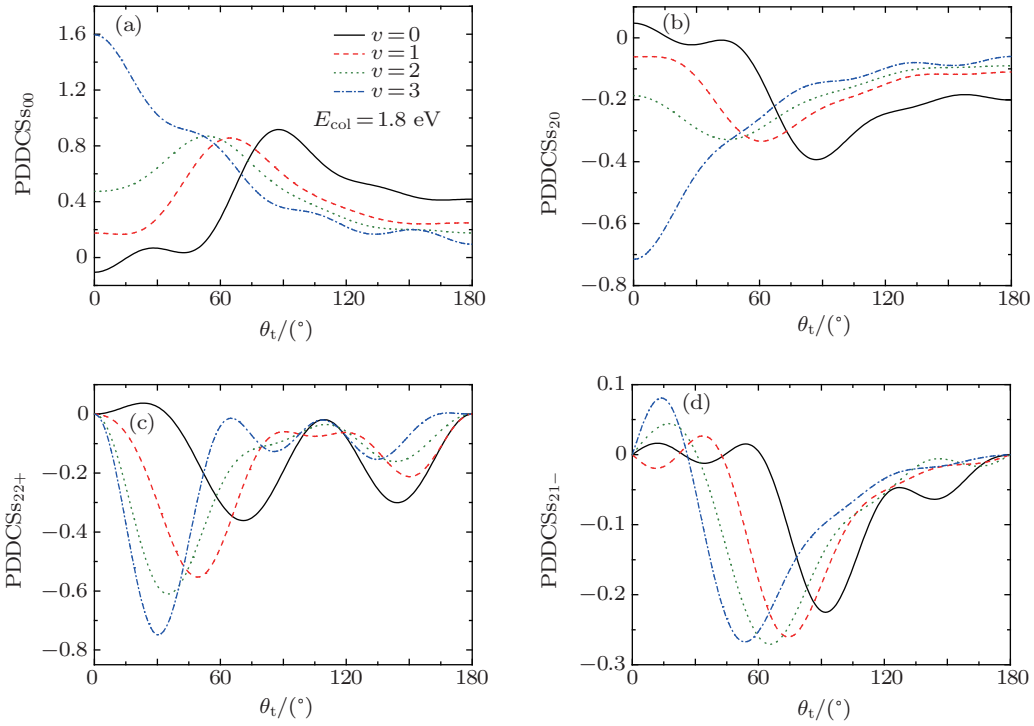


Fig. 8. (color online) Polarization-dependent differential cross sections for the reactions S (^{3}P) + H_2 ($v = 0$–3, $j = 0$) → HS + H at $E_{col} = 1.8$ eV. (a) $PDDCSs_{00}$, (b) $PDDCSs_{20}$, (c) $PDDCSs_{22+}$, (d) $PDDCSs_{21-}$.

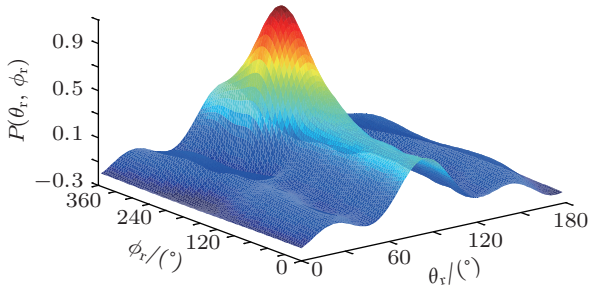


Fig. 9. (color online) $P(\theta_r, \phi_r)$ distribution for the reaction S (^{3}P) + H_2 → HS + H in the rovibrational state ($v = 0$, $j = 0$) at $E_{col} = 1.8$ eV.

Figure 9 shows the $P(\theta_r, \phi_r)$ distributions for the reagent vibrational and rotational state ($v = 0$, $j = 0$) of the title reaction at $E_{col} = 1.8$ eV. Obviously, there is only one peak at $(\theta_r, \phi_r) = (90°, 270°)$, which is in accordance with the previous discussion according to the distributions of $P(\theta_r)$ and $P(\phi_r)$. The $P(\theta_r, \phi_r)$ distribution further confirms the stereodynamics information of the title reaction. Moreover, the product of the title reaction is preferentially polarized in the direction perpendicular to the scattering plane and rotates counterclockwise in the plane which is parallel to the scattering plane. The $P(\theta_r, \phi_r)$ distributions at the other rovibrational states ($v = 1$–3, $j = 1$–3) can provide similar stereodynamics information, which is not given here.

4. Conclusion

We first use the QCT method to study the stereodynamics for the reaction S (^{3}P) + H_2 at $E_{col} = 1.8$ eV. It is found that the QCT result about the reaction probability and the integral cross section for the title reaction are highly consistent with the corresponding QM results presented by Lü *et al*. We investigate the distributions of $P(\theta_r)$, $P(\phi_r)$, $P(\theta_r, \phi_r)$, and the normalized $PDDCS_{00,20}$ on the LZHH PES. The influences of the vibrational and rotational excitation of the reagent molecule H_2 on the stereodynamics are also investigated. The calculated result shows that the product SH exhibits a rather

strong alignment perpendicular to the scattering z–x plane and a strong orientation pointing to the negative y axis. The $P(\theta_r)$ and $P(\phi_r)$ distributions show that the alignment degree of the product decreases with the increase of j or v, besides, the rotation of the product HS has a preference of changing from the in-plane reaction mechanism to the out-of-plane's mechanism with the increase of the rovibrational excitation of reagent. The $PDDCS_{00,20}$ indicates that the title reaction tends to the backward scattering as j increases from 0 to 3, however, the title reaction changes from the side-backward scattering to the forward scattering as v increases from 0 to 3. Calculations also show that the product polarization is very sensitive to the vibrational excitation of the product.

Acknowledgment

All calculations were carried out in the Shuguang Super-Computer Center (SSCC) of Ludong University. The authors thank Prof. Han Ke-Li for providing the computational codes, and also thank Dr. Lü Shuang-Jiang for providing the potential energy surface.

References

[1] Garton D J, Minton T K, Maiti B, Troya D and Schatz G C 2003 *J. Chem. Phys.* **118** 1585
[2] Maiti B and Schatz G C 2003 *J. Chem. Phys.* **119** 12360
[3] Chu T S, Zhang X and Han K L 2005 *J. Chem. Phys.* **122** 214301
[4] Han B R and Zheng Y J 2011 *J. Comput. Chem.* **32** 3520
[5] Martin R L 1983 *Chem. Phys.* **82** 337
[6] Maiti B, Schatz G C and Lendvay G 2004 *J. Phys. Chem. A* **108** 8772
[7] Klos J A, Dagdigian P J and Alexander M H 2007 *J. Chem. Phys.* **127** 154321
[8] Woiki D and Roth P 1994 *J. Phys. Chem.* **98** 12958
[9] Shiina H, Oya M, Yamashita K, Miyoshi A and Matsui H 1996 *J. Phys. Chem.* **100** 2136
[10] Chu T S, Han K L and Schatz G C 2007 *J. Phys. Chem. A* **111** 8286
[11] Lü S J, Zhang P Y, Han K L and He G Z 2012 *J. Chem. Phys.* **136** 094308
[12] Lü S J, Zhang P Y, Zhao M Y and He G Z 2012 *Comput. Theor. Chem.* **997** 83
[13] Han K L, He G Z and Lou N Q 1996 *J. Chem. Phys.* **105** 8699
[14] Li R J, Han K L, Li F E, Lu R C, He G Z and Lou N Q 1994 *Chem. Phys. Lett.* **220** 281
[15] Knowles P J and Werner H J 1985 *Chem. Phys. Lett.* **115** 259
[16] Werner H J and Knowles P J 1985 *J. Chem. Phys.* **82** 5053
[17] Knowles P J and Werner H J 1988 *Chem. Phys. Lett.* **145** 514
[18] Werner H J and Knowles P J 1988 *J. Chem. Phys.* **89** 5803
[19] Knowles P J and Werner H J 1992 *Theor. Chim. Acta* **84** 95
[20] Werner H J, Knowles P J, Lindh R, Manby F R, Schütz M, Cleani P, Korona T, Rauhut G, Amos R D, Bernhardsson A, Berning A, Cooper D L, Deegan M J O, Dobbyn A J, Eckert F, Hampel C, Hetzer G, Lloyd A W, McNicholas S J, Meyer W, Mura M E, Nicklass A, Palmieri P, Pitzer P, Schumann U, Stoll H, Stone A J, Tarroni R and Thorsteinsson T, MOLPRO, version 2006.1, a package of *ab initio* programs, 2006 see http: //www.molpro.net.
[21] Kendall P A, Dunning T H and Harrison R J 1992 *J. Chem. Phys.* **96** 6796
[22] Li X H, Wang M S, Pino H, Yang C L and Ma L Z 2009 *Phys. Chem. Chem. Phys.* **11** 10438
[23] Han K L, Zhang L, Xu D L, He G Z and Lou N Q 2001 *J. Phys. Chem. A* **105** 2956
[24] Wang M L, Han K L and He G Z 1998 *J. Phys. Chem. A* **102** 10204
[25] Chen M D, Han K L and Lou N Q 2003 *J. Chem. Phys.* **118** 4463
[26] Ren T Q 1999 *Chin. Phys.* **8** 434
[27] Zhao J, Xu Y and Meng Q T 2010 *Chin. Phys. B* **19** 063403
[28] Aoiz F J, Brouard M and Enriquez P A 1996 *J. Chem. Phys.* **105** 4964
[29] Chen M D, Han K L and Lou N Q 2002 *Chem. Phys. Lett.* **357** 483
[30] Liu L S and Shi Y 2011 *Chin. Phys. B* **20** 013404
[31] Xu Z H, Zong F J, Han B R, Dong S H, Liu J Q and Ji F 2012 *Chin. Phys. B* **21** 093103